

Metal slab superlens—negative refractive index versus inclined illumination: discussion

LUIS GRAVE DE PERALTA^{1,2}

¹Department of Physics, Texas Tech University, Lubbock, Texas 79409, USA

²Nano Tech Center, Texas Tech University, Lubbock, Texas 79409, USA (luis.grave-de-peralta@ttu.edu)

Received 22 May 2015; revised 8 August 2015; accepted 9 August 2015; posted 11 August 2015 (Doc. ID 241456); published 31 August 2015

I describe experiments using a combination of an optical microscope and a plasmonic ultrathin condenser (UTC). The UTC's structure is similar to the original proposal of a silver slab superlens. I show that the observed improvement in image resolution is determined by the well-known equation describing the resolution obtainable when a condenser is included in the microscope setup. I argue that the described experiments indicate that the so-called metal slab superlens is better described as a novel ultrathin microscope condenser, and the observed improvement in resolution is due to the illumination of the object under observation with inclined light produced by the plasmonic UTC. Implications of this opinion for the development of an optical nanoscope based on plasmonic UTCs are presented. © 2015 Optical Society of America

OCIS codes: (180.0180) Microscopy; (240.6680) Surface plasmons; (350.5730) Resolution; (110.2990) Image formation theory.

<http://dx.doi.org/10.1364/JOSAA.32.001729>

1. INTRODUCTION

Almost fifteen years ago, a thin slab of a metal, such as silver, gold, or copper, was proposed for realizing a “superlens” [1]. At the frequency of visible light, the proposed metal slab superlens was supposed to behave similar to a slab of negative refractive index material that has the power to focus all Fourier components of a two-dimensional image [1,2]. Consequently, it was predicted that a metal slab superlens should be able to resolve objects only a few nanometers across [1,3]. This prediction started a quest for optical nanoscopes based on superlenses [3–13]. However, optical nanoscopes based on negative refractive index superlenses are still outstanding. Meanwhile, last year the Nobel Prize in chemistry was awarded for the development of super-resolved fluorescence nanoscopy [14–16]. Today, near-field [17] and far-field [14–16] optical nanoscopes with resolutions of ~20 nm are commercially available; however, in order to surpass the Rayleigh resolution limit of diffraction-limited optical microscopes [18–20], available near-field and far-field optical nanoscopes often require sample fluorescence tagging, scanning, acquisition of multiple images, and intensive numerical processing [14–17]. In addition, tagging and near-field detection may disturb the object under observation during the imaging acquisition process. In contrast, traditional optical microscopes are simple to use and often permit nondisturbed, direct (no numerical postprocessing), wide-field (no scanning), and therefore fast images. Consequently, simple alternative methods for obtaining optical images with resolutions smaller than the Rayleigh resolution limit are still permitted. In particular, the use of superlenses [3–13] and more specifically

far-field superlenses [7–11,13] has been envisioned as a promising approach to realize an optical nanoscope that can be used simply as a traditional optical microscope. In this work, we present a discussion about the possibility of realizing this vision.

Since it was proposed that a thin slab of metal, such as silver or gold, may be used as a “superlens,” whose working principle is related to the negative refraction index [2,21], the possibility has attracted both support [2–13] and criticism [22–29] from numerous researchers. For instance, the experimental observation of enhanced transmission of light through a silver or gold slab [30–32] was considered in agreement with the metal slab superlens proposal [30,32]. However, this interpretation has been challenged and the same experimental results were explained as an application of the well-known phenomenon of surface plasmon resonance, without involving the concept of negative refraction [25,31]. Early demonstration of image resolution larger than 100 nm using a silver slab [4] was considered a successful demonstration of the metal slab superlens proposal [2,4,11]. The lack of a resolution of only a few nanometers was attributed to fabrication imperfections. This point of view seems to be validated by experimental results obtained with a smooth metal slab [12]. However, this particular result has not been validated by further experiments; moreover, several reported resolution values obtained using “superlenses” are no better than the resolution that could be obtained using common microscope condensers [26–29]. The apparent failure of the “superlens promise” could then be understood as a corroboration of critiques arguing that the negative refraction of the metal slab does not guarantee super-resolution [22–24] or,

alternatively, as a corroboration of critiques arguing that negative refraction is not the cause of the resolution improvement reported in experiments with metal slabs [25–28]. For instance, it is well known that microscope condensers improve the resolution of an optical microscope simply by illuminating the sample with inclined illumination without the need for sample fluorescence tagging, scanning, or acquisition of multiple images [33–35]. When a coherent beam of light impinges perpendicular to the sample in a traditional optical microscope, the minimum observable period is $p_{\min} \sim \lambda/\text{NA}_o$ [18–20], where λ is the wavelength of the illumination source in vacuum and NA_o is the numerical aperture of the microscope objective lens. Illuminating the sample with very wide angles, provided by a condenser, improves the microscope resolution and reduces p_{\min} to $\sim \lambda/(2\text{NA}_o)$ [18–20,28,33], which is the well-known Rayleigh resolution limit of diffraction-limited imaging instruments [18–20,33,34]. The achievable resolution of an optical microscope using a microscope condenser with numerical aperture NA_c is given by the following expression [28,33]:

$$p_{\min} = \frac{\lambda}{\text{NA}_o + \text{NA}_c}. \quad (1)$$

From Eq. (1) it follows that the Rayleigh resolution limit occurs when $\text{NA}_c = \text{NA}_o$ [33]. Traditional microscope condensers consist of a combination of bulky lenses (or mirrors) and diaphragms designed to illuminate the sample with a cone of inclined light. However, digital condensers with no lenses, mirrors, or moving parts [29,36–38]; plasmonic ultrathin condensers (UTC) [13,28,32,39]; and more general UTCs occupying a volume three orders of magnitude smaller than bulky condensers [26–28] have been recently reported. Equation (1) supports the hope for a single-shot, far-field, non-scanning path toward an optical nanoscope because it suggests that is possible to surpass the Rayleigh resolution limit using microscope condensers with $\text{NA}_c \gg \text{NA}_o$ [37–40]. For instance, this was recently demonstrated at $\lambda = 570$ nm by resolving the structure of a plasmonic crystal with square symmetry and period of 550 nm, using a traditional optical microscope with a $\text{NA}_o = 0.25$ objective lens in combination with a plasmonic UTC with $\text{NA}_c \sim 1.1$ [39]. However, as in commercialized optical nanoscopy methods, numerical processing was necessary for the reported resolution improvement [39,40].

Using experimental results obtained in our research group, in this work I argue in favor of the opinion that observed improvements in image resolution obtained using far-field “superlenses,” based on variations of the original metal slab proposal, can be better explained describing the so-called far-field superlenses as plasmonic UTCs. This paper is organized as follows. In Section 2, experiments previously reported by our research group are discussed. In addition, new experiments are presented demonstrating that objects under observation do not need to be in the near field of the metal layer to be imaged by the metal slab with improved resolution. I argue that the observed improvement in resolution is due to the illumination of the object under observation by the inclined light produced by the plasmonic UTCs. In Section 3, I discuss the implications of this opinion for the possibility of developing optical nanoscopes based on plasmonic UTCs that can be used simply as

traditional optical microscopes. Finally, the conclusions of this work are presented in Section 4.

2. EXPERIMENTS USING PLASMONIC UTC

Figure 1 illustrates the structure of the samples used in this work and in previously reported experiments. A plasmonic UTC [28], sketched in Fig. 1(a), consists of a multilayered structure that was fabricated on a glass coverslip. The 150 μm thick coverslip serves as the substrate onto which a 2 nm thick Cr adhesion layer is deposited, using e-beam evaporation, followed by a 45 nm thick Au layer. Finally, an ~ 110 nm layer of poly-methyl-methacrylate (PMMA) doped with rhodamine-6G (R6G) is spin coated on top of the gold layer. The R6G dopant is a fluorescent material that has peak absorption/emission at 532/568 nm and, when pumped with a laser, serves as a surface plasmon polariton (SPP) [41] excitation source. The excited SPPs propagate along the PMMA/Au interface before leaking down toward the glass substrate [30–32]. The object under observation in the sample arrangement schematics shown in Figs. 1(b) and 1(c) is a square array of Cr pillars that is placed in the far [Fig. 1(b)] or near [Figs. 1(c) and 1(d)] field of the UTC's emission layer.

Figure 2 shows a schematic of the Nikon Eclipse Ti inverted microscope used in our experiments [13,26–28,32,39], which were carried out using the following procedure. A fiber-coupled, continuous-wave, 532 nm wavelength solid-state laser was used to illuminate the UTC and pump the R6G fluorescent material, which in turn excites SPPs. The leakage radiation coupled to the excited SPPs was captured by the oil-immersion objective lens [32,42]. It is worth noting that when the plasmonic UTC sketched in Fig. 1(c) is placed in the microscope setup sketched in Fig. 2, the UTC is basically the originally proposed metal slab “superlens” [1,2] but is used in a variation of the Kretschmann configuration, where the first lens of the oil-immersion objective lens functions as the glass prism [2–4,32].

All the light collected by the objective lens is directed through either a $\Delta\lambda = 10$ nm bandpass filter centered at the $\lambda = 570$ nm wavelength or a long-pass filter rated to transmit light of $\lambda > 570$ nm wavelengths, both of which spectrally filter out the transmitted laser light and allow the leakage radiation to be detected by the microscope. The leakage radiation passes through a set of internal lenses that direct it toward a

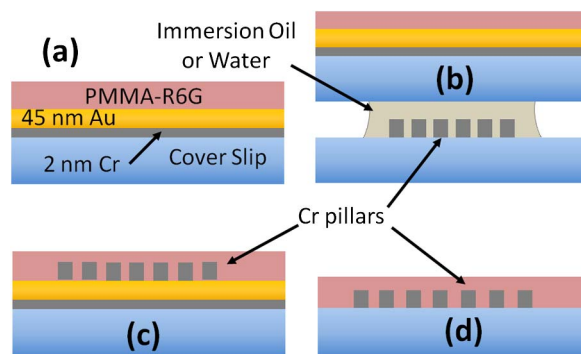


Fig. 1. Schematic (not to scale) of the transversal structures of (a)–(c) plasmonic UTCs and (d) a nonplasmonic UTC. Cr pillars are in the (b) far and (c) near field of the metal slab.

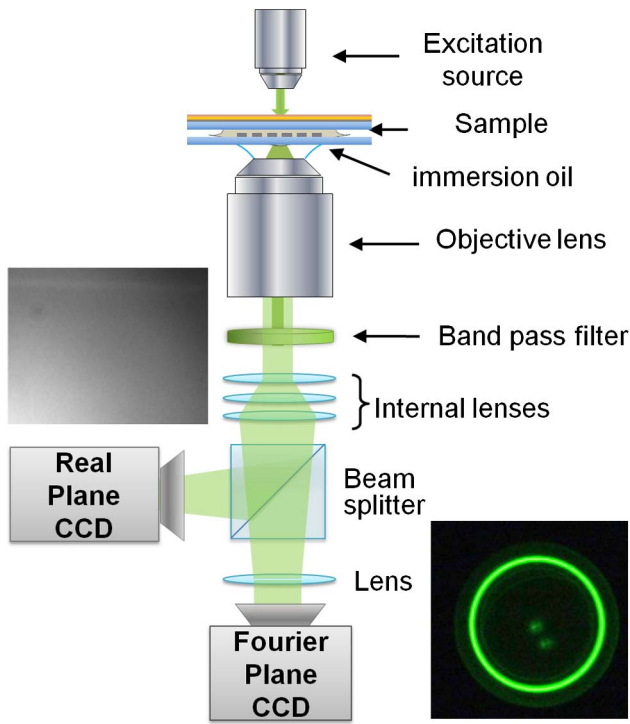


Fig. 2. Schematic (not to scale) of the microscope setup. The insets are instances of RP and FP images corresponding to a sample like the sketch in Fig. 1(a).

beam splitter which will then send the light to a real plane (RP) charge-coupled device (CCD) camera or through another lens, which takes the Fourier transform of the light, and then to a Fourier plane (FP) CCD camera. The RP camera captures an image of the sample as it is seen through the microscope's eyepiece, while the FP camera images the momentum distribution of the leakage radiation emitted by the UTC [13,26–28,32,39]. As shown in the inset of Fig. 2, when the sample is a plasmonic UTC, as sketched in Fig. 1(a), the FP image is formed by one or more concentric bright rings [32] and, as expected, the RP image shows the uniform surface of the PMMA layer. The spontaneous photons emitted by the R6G excited molecules that passed directly through the UTC's gold layer without exciting SPPs produce the background in the FP image; however, the bright ring observed in the FP image is produced by the photons that excited SPPs and then leaked to the microscope objective [31,32]. The observation of bright rings in the FP has been interpreted as evidence of the prediction, related to the negative refractive index concept [1,2], of the rapid growth of evanescent waves in a metal slab [30]. However, a less dramatic but simple explanation is that the observed transmission enhancement is due to the nature of SPPs [25]. In any case, the observation of the bright rings in the FP images indicates that the more probable pathway for a spontaneous emission photon to pass through the metal slab is by exciting a SPP. These photons leak to the oil-immersion objective lens in a highly inclined direction with respect to the normal to the metal surface.

Consequently, the plasmonic UTC could be used in a microscope as a condenser, i.e., as a source of far-field inclined light for illuminating the object under observation. Moreover,

because leakage radiation occurs at inclination angles larger than the total internal reflection angle, UTCs have values of $NA_c > 1$ [13,28,39]. In order to study this possibility, a sample with the structure sketched in Fig. 1(b) was prepared and placed in the microscope setup as illustrated in Fig. 2. The top part of the stacked sample arrangement sketched in Fig. 1(b) is the plasmonic UTC sketched in Fig. 1(a). The bottom part of the sandwich is another coverslip separated by liquid (water or index-matching oil) from the UTC. The object to be observed is an array of 15 nm tall Cr pillars fabricated on top of the bottom coverslip in a square lattice arrangement with a period of $p = 300$ nm; therefore, the Cr pillars are hundreds of micrometers away from the metal slab. Consequently, when the sample is placed in the microscope arrangement sketched in Fig. 2, the Cr pillars are illuminated by far-field leakage radiation emanated from the metal slab. Figure 3 shows FP and RP images corresponding to the stacked sample that were obtained with a bandpass filter centered at $\lambda = 570$ nm and a $NA_o = 1.3$ 100× objective lens. Figures 3(a) and 3(b) correspond to an arrangement using index-matching oil and Figs. 3(c) and 3(d) to an arrangement using water. Centered concentric and a portion of shifted rings are clearly observed in the FP images seen in Figs. 3(a) and 3(c) [13,28,39,40]. The radius of the inner concentric ring is equal to the radius of the shifted rings indicating that the observed rings are the condenser features responsible for the increased resolution ability of the UTC [13,28,39,40]. Therefore, the central ring is the zeroth-order diffraction ring and the shifted rings are the first-order diffraction rings, which follow the same square symmetry of the patterned holes. The boundary of the disk-like background in the FP images corresponds to the objective lens NA_o [32,43]. This permits one to find out the value of NA_c of the plasmonic UTC as $NA_c = NA_o \cdot r_{SPP} / r_{max}$, where r_{SPP} and r_{max} are the radii of the diffraction rings and the disk-like boundary in the FP images, respectively [43]. By this approach, we determined $NA_c \sim 1.1$ from both FP images in Figs. 3(a) and 3(c). It is

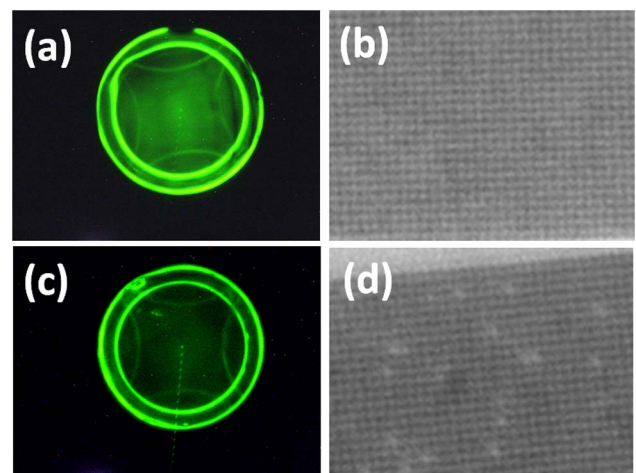


Fig. 3. (a), (c) FP and (b), (d) RP images of Cr pillars in a square lattice arrangement with $p = 300$ nm obtained using the stacked sample arrangement sketched in Fig. 1(b) with (a), (b) oil and (c), (d) water in between the UTC and the separate coverslip. The images were taken using a bandpass filter centered at $\lambda = 570$ nm and a $NA_o = 1.3$ 100× objective lens.

no surprise then that the square lattice patterned on the sample is visible in the RP images shown in Figs. 3(b) and 3(d), since the minimum observable period calculated using Eq. (1) is $p_{\min} = 238 \text{ nm} < p$. This is in excellent agreement with the observation of both zeroth- and first-order diffraction rings in the FP image shown in Fig. 3(a) [13,39,40]. Nevertheless, it should be noted that $\lambda/\text{NA}_o = 438 \text{ nm}$ for $\lambda = 570 \text{ nm}$ and $\text{NA}_o = 1.3$. Therefore, a periodical structure with $p = 300 \text{ nm}$ should not be visible under perpendicular illumination.

It is worth noting that first, while resolution is improved with respect to the obtainable resolution using perpendicular illumination, observed periodicity was larger than $\lambda/(2\text{NA}_o)$. Second, being the object under observation in the far field of the UTC's gold layer, the object did not interact directly with the SPPs excited in the UTC but with the leakage radiation emitted by the UTC. Third, the negative refractive index concept is not necessary to explain the experimental results presented in Fig. 3. This is because observed improvement in resolution was produced by the illumination of the object under observation with highly inclined leakage radiation coming from the UTC. The successful demonstration of the resolution enhancement provided by a plasmonic UTC condenser, in a stacked sample arrangement with a water medium placed in between the UTC and a common coverslip, suggests that a plasmonic UTC can be used to image three-dimensional objects with a thickness of several microns in an aqueous solution. This is not possible with common plasmonic microscopy techniques, which are used for imaging a thin layer of the object under observation close to the metal with improved resolution [44,45]. This attribute opens the door for the use of UTCs to image biomedical samples. To test this exciting possibility, a drop of human blood was placed on a coverslip. Then a plasmonic UTC was placed on top of the blood in a stacked sample arrangement. In this arrangement, the objects to be studied are the cells that are immersed in the blood plasma—a solution that is 95% water. The images obtained using a $\text{NA}_o = 1.3$ 100 \times objective lens are shown in Fig. 4. The RP image shown in Fig. 4(a) was obtained using the leakage radiation produced by the UTC. Figure 4(b) shows the corresponding FP image. Both images featured in Fig. 4 were obtained using a long-pass filter instead of a bandpass filter. This procedure was carried out to allow more light to be captured by the RP and FP cameras, which allowed for shorter exposure times ($\Delta t \sim 100 \text{ ms}$)—a necessary feature when imaging dynamic live structures. Both the bandpass and long-pass filters are rated for a minimum transmitted wavelength of $\lambda = 570 \text{ nm}$; as such, similar resolution enhancements, compared to the experiments using the bandpass filter, can be obtained in this arrangement since the lowest wavelength captured determines the smallest resolution feature. The FP image in Fig. 4(b) shows the characteristic zeroth-order diffraction ring with $\text{NA}_c > 1$ produced by the plasmonic UTC. The lack of first-order diffraction rings is expected since the object being studied is not periodic. The diffuse broad bright center in Fig. 4(b) is produced by the contribution of the low spatial frequencies corresponding to the micrometer-size dimensions of the cells clearly observed in the RP image shown in Fig. 4(a). The good quality of the RP image demonstrates that the originally proposed metal slab “superlens” [1,2,30], in a

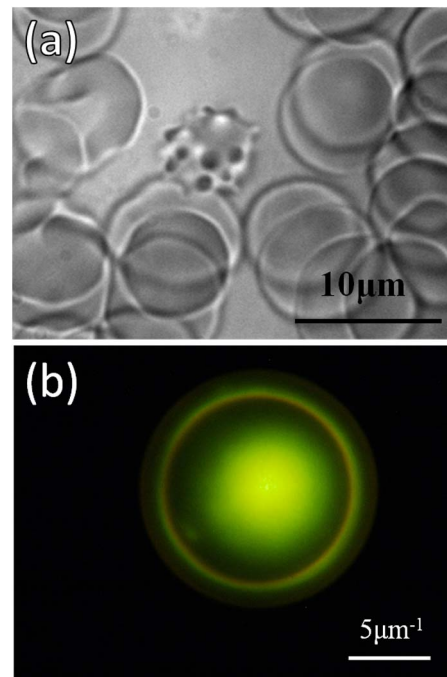


Fig. 4. (a) RP and (b) FP images of human blood sandwiched in a stacked sample arrangement. The FP image was taken using a long-pass filter rated to transmit all wavelengths $\lambda > 570 \text{ nm}$ and a $\text{NA}_o = 1.3$ 100 \times objective lens.

plasmonic UTC arrangement, can be used as a microscope condenser with large numerical aperture ($\text{NA}_c > 1$) for illuminating objects with a thickness of several microns placed at the far field of the illumination source (UTC). This is in clear opposition with the opinion that the improvement in image resolution provided by the proposed metal slab “superlens” is related to the negative refraction index concept and is due to its power to focus all Fourier components including the evanescent ones [1,2,30]. In our research group, we previously demonstrated similar image resolution improvements using plasmonic UTCs when the objects under observation were illuminated with excited SPPs propagating in the surface of the metal slab [13,28]. In these experiments, a sample structure similar to the sketch in Fig. 1(c) was imaged using the microscope setup sketched in Fig. 2. Initially, we described the observed resolution improvement in terms of far-field “superlenses” related to the negative refraction concept [13,32,43]; however, the discovery of nonplasmonic UTCs [26] made it clear that a negative refractive index was not related to the observed improvement in resolution [27,28]. A sample with the structure sketched in Fig. 1(d) cannot be considered at all a “superlens” related to the negative refraction concept because it has no metal layer. Nevertheless, similar resolution improvements were obtained for plasmonic and nonplasmonic UTCs using the same microscope setup sketched in Fig. 2 [27,28]. FP images are formed by light diffracted by the object under observation. Under perpendicular illumination, the zeroth-order diffraction spot appears at the center of the FP images [18–20,40]. However, the zeroth-order diffraction spot appears shifted in the FP images when inclined illumination is used

[20]. When a microscope condenser is used, rings formed by a multitude of diffraction spots shifted in all directions are observed in the FP images [27,39,40]. The observation of rings in the FP images is the common image formation principle when plasmonic [Fig. 1(c)] and nonplasmonic [Fig. 1(d)] UTCs are used for imaging an object that is in the near [Figs. 1(c) and 1(d)] or far [Fig. 1(d)] field of the surface emitting leakage radiation. These rings are formed by diffracted light. The zeroth-order diffraction ring observed in a FP image indicates that the corresponding diffraction pattern contains shifted zeroth-order diffraction spots, which are characteristic of diffraction patterns formed under inclined illumination. Consequently, one can conclude that inclined illumination explains why similar resolution values are obtained with plasmonic and nonplasmonic UTCs independently of the position of the object. This also explains why the resolution limit for microscopes using UTCs is given by Eq. (1) [13,28]. As discussed above, one does not need the negative refraction index concept to explain experimental results that are obtained using plasmonic UTCs for imaging objects, which are placed at the far field of the UTC's metal layer. Inclined emission of leakage radiation by the UTC is also the cause of observed improvement in resolution when the object is in the near field of the UTC's emission layer.

3. DISCUSSION

The quest for an optical nanoscope based on far-field superlenses related to the negative refractive index concept [3–13] may then continue as the search for an optical nanoscope based on inclined illumination produced by microscope condensers. However, it is well known that in practice, the achievable resolution using microscope condensers cannot be notably reduced below the Rayleigh resolution limit just by making $NA_c \gg NA_o$ [33]. This is illustrated in Fig. 5, which shows images of a sample with the structure sketched in Fig. 1(c) and $p = 350$ nm obtained using the microscope setup sketched in Fig. 2. The images were obtained with a bandpass filter

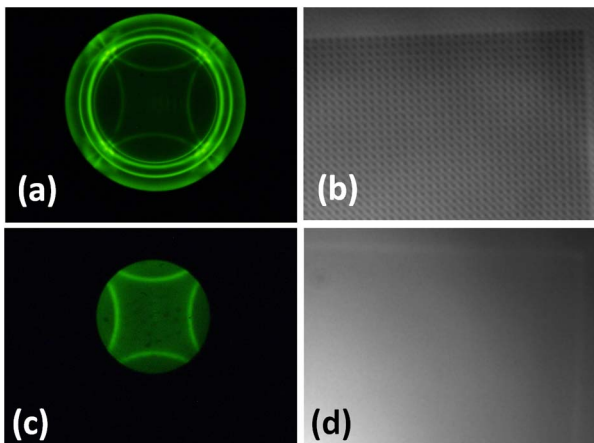


Fig. 5. (a), (c) FP and (b), (d) RP images of Cr pillars in a square lattice arrangement with $p = 350$ nm obtained using the sample arrangement sketched in Fig. 1(c). The images were taken using a bandpass filter centered at $\lambda = 570$ nm and a $100\times$ objective lens with $NA_o =$ (a), (b) 1.3 and (c), (d) 0.9.

centered at $\lambda = 570$ nm and by using two different objective lenses with the same $100\times$ magnification. Figures 5(a) and 5(b) [Figs. 5(c) and 5(d)] show FP and RP images obtained with $NA_o = 1.3$ (0.9), respectively. Portions of four first-order diffraction rings with the square symmetry of the Cr pillar array can be observed in both FP images shown in Fig. 5; however, the zeroth-order diffraction ring can be observed only in the FP image obtained with $NA_o > NA_c \sim 1.1$ [Fig. 5(a)]. Two consecutive orders of diffraction must be observed in the FP image in order to resolve the Cr structure in the RP image [39,40]; consequently, the Cr array is only visible in the RP image shown in Fig. 5(b).

Nevertheless, it has been recently demonstrated that as long as first-order diffraction features are collected by the microscope objective lens, by numerically reconstructing a synthetic FP image with numerical aperture $NA_s = NA_o + NA_c$, it is possible to recover the RP image when $NA_c \gg NA_o$ [37–40]. Consequently, the minimum resolvable period using an optical microscope based on inclined illumination produced by microscope condensers is proportional to λ/N_s [38,39]; therefore, such a nanoscope would not produce direct images because (i) further imaging numerical postprocessing would be necessary and (ii) a condenser with $NA_c \gg 1$ is necessary for realizing such an optical nanoscope, which would not be a fluorescence nanoscope because the light used for imaging in a condenser-based optical nanoscope would be light diffracted by the object under observation. This imposes a fundamental physics limitation to the possible realization of such a nanoscope. It is well known that if a periodically patterned sample is immersed in a medium with refractive index n and the sample is illuminated uniformly, interference between light diffracted in the same direction by different regions of the object can only occur when the period of the sample is larger than half of the wavelength of the light in the medium, i.e., $p > \lambda/(2n)$ [29,46,47]. This seems to put a fundamental limit to the validity of Eq. (1). For instance, a value of $p_{\min} = 180$ nm, obtained from Eq. (1) when $NA_c = NA_o = n$, was reached using a hemispherical digital condenser in combination with $n \sim 1.5$ and $\lambda = 540$ nm [29]. Nevertheless, structured illumination microscopy cuts this limit in half [48–50]. This is because Eq. (1) and the so-called linear systems limit of optical resolution, $\lambda/(2n)$ [46], are only valid when the sample is uniformly illuminated [48,49]. For instance, when a large uniform sample is uniformly illuminated, the intensity in the FP image is only large in a small spot at the center of the image [40]. However, an interference pattern is formed in the microscope's FP when a uniform sample is illuminated with a periodical intensity distribution [51]. Summarizing, the achievable resolution of an optical microscope based on microscope condensers and using structured illumination in combination with large synthetic NA_s techniques is given by the following expression:

$$p_{\min} \sim \frac{\lambda}{2(NA_o + NA_c)}. \quad (2)$$

Assuming $NA_o \sim NA_c \sim n \sim 1.5$ and $\lambda \sim 570$ nm, Eq. (2) gives a value of $p_{\min} \sim \lambda/(4n) \sim 95$ nm. Consequently, realizing a nanoscope with image resolution of ~ 20 nm still requires a four times improvement. This could be achieved using a nonlinear medium [41,49]. In particular, the nonlinear

dispersion of the SPPs excited in the metal/dielectric interface in a variation of or in the original metal slab proposal could provide the required nonlinearity. For instance, due to the nonlinear dispersion of plasmonic resonances [41], the effective refractive index of excited SPPs, n_{eff} , could be much larger than n in a plasmonic UTC with the structure sketched in Fig. 1(a) but with glass substituted by another material like GaP, which is nonmetallic and transparent and has $n > n_{\text{glass}} \sim 1.5$. In a plasmonic UTC with the homogeneous and featureless structure sketched in Fig. 1(a), due to momentum conservation, excited SPPs with $n_{\text{eff}} > n$ could not be used for far-field illumination, as described above in Section 2, because such dark SPPs could not leak to the objective lens of the microscope. However, nanosize objects in the near field of the metal/nonmetal interface [Fig. 1(c)] may scatter the excited SPPs. Collecting with the nanoscope objective lens, the light scattered by a periodical structure may result in FP images similar to the FP image shown in Fig. 5(c), from where the RP image of the nanosize objects can be reconstructed using large synthetic NA techniques [37–40].

4. CONCLUSIONS

I argue that most of the demonstrated far-field superlenses based on variations of the so-called metal slab “superlens” are better described as microscope condensers. I have presented experiments demonstrating that a variation of the originally proposed metal slab “superlens” works as a far-field source of inclined illumination. Illumination of the object under observation with inclined light explains the observed improvement in image resolution. I also discussed previously reported experiments that demonstrate the hypothesis of negative refraction index is not needed for explaining similar improvements in image resolution obtained using UTCs. Finally, I show that the identification of far-field “superlenses” as plasmonic UTCs permits the quest for optical nanoscopes that are not based on fluorescence but on plasmonic UTCs with extremely large values of NA_c . I argue that it is worthy to work toward this objective (i) because it is within reach and (ii) because optical nanoscopes based on plasmonic UTCs will be simple to use and will permit far-field, nondisturbed, wide-field images of non-tagged samples.

REFERENCES

- J. B. Pendry, “Negative refraction makes a perfect lens,” *Phys. Rev. Lett.* **85**, 3966–3969 (2000).
- J. B. Pendry, “Negative refraction,” *Contemp. Phys.* **45**, 191–202 (2004).
- D. O. S. Melville, R. J. Blaikie, and C. R. Wolf, “Submicron imaging with a planar silver lens,” *Appl. Phys. Lett.* **84**, 4403–4405 (2004).
- D. O. S. Melville and R. J. Blaikie, “Super-resolution imaging through a planar silver layer,” *Opt. Express* **13**, 2127–2134 (2005).
- S. Durant, Z. Liu, J. M. Steele, and X. Zhang, “Theory of the transmission properties of an optical far-field superlens for imaging beyond the diffraction limit,” *J. Opt. Soc. Am. B* **23**, 2383–2392 (2006).
- J. B. Pendry and D. R. Smith, “The quest for the superlens,” *Sci. Am.* **295**, 60–67 (2006).
- Z. Liu, S. Durant, H. Lee, Y. Pikus, N. Fang, Y. Xiong, C. Sun, and X. Zhang, “Far-field optical superlens,” *Nano Lett.* **7**, 403–408 (2007).
- Z. Liu, S. Durant, H. Lee, Y. Pikus, Y. Xiong, C. Sun, and X. Zhang, “Experimental studies of far-field superlens for sub-diffractive optical imaging,” *Opt. Express* **15**, 6947–6954 (2007).
- Z. Liu, H. Lee, Y. Xiong, C. Sun, and X. Zhang, “Far-field optical hyperlens magnifying sub-diffraction-limited objects,” *Science* **315**, 1686 (2007).
- I. I. Smolyaninov, Y. J. Hung, and C. C. Davis, “Magnifying superlens in the visible frequency range,” *Science* **315**, 1699–1701 (2007).
- X. Zhang and Z. Liu, “Superlenses to overcome the diffraction limit,” *Nat. Mater.* **7**, 435–441 (2008).
- P. Chaturvedi, W. Wu, V. J. Logeeswaran, Z. Yu, M. S. Islam, S. Y. Wang, R. S. Williams, and N. X. Fang, “A smooth optical superlens,” *Appl. Phys. Lett.* **96**, 043102 (2010).
- C. J. Regan, R. Rodriguez, S. Gourshetty, L. Grave de Peralta, and A. A. Bernussi, “Imaging nanoscale features with plasmon-coupled leakage radiation far-field superlenses,” *Opt. Express* **20**, 20827–20834 (2012).
- S. W. Hell and M. Krough, “Ground-state depletion fluorescence microscopy, a concept for breaking the diffraction resolution limit,” *Appl. Phys. B* **60**, 495–497 (1995).
- T. A. Klar, S. Jakobs, M. Dyba, A. Egner, and S. W. Hell, “Fluorescence microscopy with diffraction resolution broken by stimulated emission,” *Proc. Natl. Acad. Sci. USA* **97**, 8206–8210 (2000).
- X. Zhuang, “Nano-imaging with STORM,” *Nat. Photonics* **3**, 365–367 (2009).
- E. Betzig, M. Isaacson, and A. Lewis, “Collection mode near field scanning optical microscopy,” *Appl. Phys. Lett.* **51**, 2088–2090 (1987).
- E. Hecht, *Optics*, 3rd ed. (Addison Wesley, 1998).
- M. Born and E. Wolf, *Principles of Optics*, 5th ed. (Pergamon, 1975).
- J. W. Goodman, *Introduction to Fourier Optics* (McGraw-Hill, 1968).
- V. G. Veselago, “The electrodynamics of substances with simultaneously negative values of ϵ and μ ,” *Sov. Phys. Usp.* **10**, 509–514 (1968).
- J. M. Williams, “Some problems with negative refraction,” *Phys. Rev. Lett.* **87**, 249703 (2001).
- N. Garcia and M. Nieto-Vesperinas, “Left-handed materials do not make a perfect lens,” *Phys. Rev. Lett.* **88**, 207403 (2002).
- M. Nieto-Vesperinas, “Problem of image superresolution with a negative-refractive-index slab,” *J. Opt. Soc. Am. A* **21**, 491–498 (2004).
- G. Christou and C. Mias, “Critique of optical negative refraction superlensing,” *Plasmonics* **6**, 307–309 (2011).
- C. J. Regan, D. Dominguez, A. A. Bernussi, and L. G. de Peralta, “Far-field optical superlenses without metal,” *J. Appl. Phys.* **113**, 183105 (2013).
- R. Lopez-Boada, C. J. Regan, D. Dominguez, A. A. Bernussi, and L. Grave de Peralta, “Fundamentals of optical far-field subwavelength resolution based on illumination with surface waves,” *Opt. Express* **21**, 11928–11942 (2013).
- D. B. Desai, D. Dominguez, A. A. Bernussi, and L. Grave de Peralta, “Ultra-thin condensers for optical subwavelength resolution microscopy,” *J. Appl. Phys.* **115**, 093103 (2014).
- L. Molina, D. Dominguez, D. B. Desai, T. O’Loughlin, A. A. Bernussi, and L. Grave de Peralta, “Hemispherical digital optical condensers with no lenses, mirrors, or moving parts,” *Opt. Express* **22**, 6948–6957 (2014).
- Z. Liu, N. Fang, T. Yen, and X. Zhang, “Rapid grow of evanescent wave by a silver superlens,” *Appl. Phys. Lett.* **83**, 5184–5186 (2003).
- I. Gryczynski, J. Malicka, Z. Gryczynski, and J. R. Lakowicz, “Surface plasmon-coupled emission with gold films,” *J. Phys. Chem. B* **108**, 12568–12574 (2004).
- S. P. Frisbie, C. Chesnut, M. E. Holtz, A. Krishnan, L. Grave de Peralta, and A. A. Bernussi, “Image formation in wide-field microscopes based on leakage of surface plasmon-coupled fluorescence,” *IEEE Photon. J.* **1**, 153–162 (2009).
- H. H. Hopkins and P. M. Barham, “The influence of the condenser on microscopic resolution,” *Proc. Phys. Soc. B* **63**, 737–744 (1950).
- H. Köhler, “On Abbe’s theory of image formation in the microscope,” *Optica Acta* **28**, 1691–1701 (2010).
- A. Vainrub, O. Pustovyy, and V. Vodyanov, “Resolution of 90 nm ($\lambda/5$) in an optical transmission microscope with annular condenser,” *Opt. Lett.* **31**, 2855–2857 (2006).

36. G. Zheng, C. Kolner, and C. Yang, "Microscopy refocusing and dark-field imaging by using a simple LED array," *Opt. Lett.* **36**, 3987–3989 (2011).
37. G. Zheng, R. Horstmeyer, and C. Yang, "Wide-field, high-resolution Fourier ptychographic microscopy," *Nat. Photonics* **7**, 739–745 (2013).
38. X. Ou, R. Horstmeyer, G. Zheng, and C. Yang, "High numerical aperture Fourier ptychography: principle, implementation and characterization," *Opt. Express* **23**, 3472–3491 (2015).
39. D. Dominguez, M. Alhusain, N. Alharbi, A. A. Bernussi, and L. Grave de Peralta, "Fourier plane imaging microscopy for detection of plasmonic crystals with periods beyond the optical diffraction limit," *Plasmonic*, doi:10.1007/s11468-015-9938-x (to be published).
40. D. Dominguez, M. Alhusain, N. Alharbi, A. Bernussi, and L. Grave de Peralta, "Fourier plane imaging microscopy," *J. Appl. Phys.* **116**, 103102 (2014).
41. H. Raether, *Surface Plasmons on Smooth and Rough Surfaces and on Gratings* (Springer-Verlag, 1988).
42. A. Drezet, A. Hohenau, D. Koller, A. Stepanov, H. Ditlbacher, B. Steinberger, F. R. Aussenegg, A. Leitner, and J. R. Krenn, "Leakage radiation microscopy of surface plasmon polaritons," *Mater. Sci. Eng. B* **149**, 220–229 (2008).
43. R. Rodriguez, C. J. Regan, A. Ruiz-Columbié, W. Agutu, A. A. Bernussi, and L. Grave de Peralta, "Study of plasmonic crystals using Fourier-plane images obtained with plasmon tomography far-field superlenses," *J. Appl. Phys.* **110**, 083109 (2011).
44. E. Yeatman and E. Ash, "Surface plasmon microscopy," *Electron. Lett.* **23**, 1091–1092 (1987).
45. G. Stabler, M. G. Somekh, and C. W. See, "High-resolution wide-field surface plasmon microscopy," *J. Microsc.* **214**, 328–333 (2004).
46. Y. Kuznetsova, A. Neumann, and S. R. J. Brueck, "Imaging interferometric microscopy approaching the linear systems limits of optical resolution," *Opt. Express* **15**, 6651–6663 (2007).
47. R. P. Feynman, R. B. Leighton, and M. Sands, *The Feynman Lectures on Physics* (Adison Wesley, 1966), Vol. **3**.
48. M. G. Gustafsson, "Surpassing the lateral resolution limit by a factor of two using structured illumination microscopy," *J. Microsc.* **198**, 82–87 (2000).
49. M. G. Gustafsson, "Nonlinear structured-illumination microscopy: Wide-field fluorescence imaging with theoretical unlimited resolution," *Proc. Natl. Acad. Sci. USA* **102**, 13081–13086 (2005).
50. S. Chowdhury, A. Dhalla, and J. Isatt, "Structured oblique illumination microscopy for enhanced resolution imaging of non-fluorescent, coherently scattering samples," *Biomed. Opt. Express* **3**, 1841–1854 (2012).
51. J. Ajimo, C. J. Regan, A. C. Bernussi, S. Park, R. Lopez-Boada, A. A. Bernussi, and L. Grave de Peralta, "Study of interference in a double-slit without walls by plasmon tomography techniques," *Opt. Commun.* **284**, 4752–4755 (2011).